Evolution of Enzymatic Activities in the Orotidine 5′-Monophosphate Decarboxylase Suprafamily: Mechanistic Evidence for a Proton Relay System in the Active Site of 3-Keto-L-gulonate 6-Phosphate Decarboxylase†

Wen Shan Yew,‡ Eric L. Wise,§ Ivan Rayment,*,§ and John A. Gerlt*,‡

Departments of Biochemistry and Chemistry, University of Illinois, Urbana, Illinois 61801, and Department of Biochemistry, University of Wisconsin, Madison, Wisconsin 53706

Received February 4, 2004; Revised Manuscript Received March 18, 2004

ABSTRACT: 3-Keto-L-gulonate 6-phosphate decarboxylase (KGPDC) and orotidine 5′-monophosphate decarboxylase (OMPDC) are homologous enzymes that share the $(\beta/\alpha)_8$-fold but catalyze mechanistically distinct reactions [Wise, E., Yew, W. S., Babbitt, P. C., Gerlt, J. A., and Rayment, I. (2002) *Biochemistry 41*, 3861−3869]. KGPDC catalyzes the Mg^{2+}-dependent decarboxylation of 3-keto-L-gulonate 6-phosphate, an intermediate in the catabolic pathway of L-ascorbate utilization by *Escherichia coli* K-12 [Yew, W. S., and Gerlt, J. A. (2002) *J. Bacteriol. 184*, 302−306]. OMPDC catalyzes a metal ion-independent reaction that likely proceeds without a vinyl anion intermediate [Appleby, T. C., Kinsland, C., Begley, T., and Ealick, S. E. (2000) *Proc. Natl. Acad. Sci. U.S.A. 97*, 2005−2010], although the mechanistic details are uncertain. An active site Lys located at the end of the third β-strand in OMPDC has been proposed to be the general acid that delivers a solvent-derived proton to the UMP product; the active site of KGPDC contains a homologous Lys residue (Lys64). Herein, we report investigations of the KGPDC-catalyzed reaction that are consistent with a mechanism involving a Mg^{2+}-stabilized *cis*-enediolate intermediate [Wise, E. L., Yew, W. S., Gerlt, J. A., and Rayment, I. (2003) *Biochemistry 42*, 12133−12142] and implicate waters proximal to His136 and Arg139, both located at the end of the sixth β-strand, as the general acids that deliver a solvent-derived proton to the intermediate to form the L-xylulose 5-phosphate product. On the basis of our mechanistic investigations, Lys64 stabilizes the *cis*-enediolate intermediate by forming hydrogen bonds to both O1 and O2 of the intermediate. Thus, although the active sites of OMPDC and KGPDC contain a conserved Lys at the end of the third β-strand, their roles in catalysis are not conserved. Furthermore, a conserved Asp at the end of the third β-strand in OMPDC participates in a hydrogen-bonded network that positions the acidic Lys residue; in the active site of KGPDC, the homologous Asp67 participates in stabilization of the enediolate intermediate and enforces a *cis* geometry. We conclude that the conserved active site residues perform different functions in the OMPDC- and KGPDC-catalyzed reactions, so the mechanisms of their reactions are completely distinct. This study further highlights the opportunistic nature of divergent evolution in conscripting the active site of a progenitor to catalyze a mechanistically distinct reaction.

In the utilization of L-ascorbate by *Escherichia coli* K-12 and other microbial species, 3-keto-L-gulonate 6-phosphate is decarboxylated to L-xylulose 5-phosphate (*1*). The enzyme that catalyzes this reaction, 3-keto-L-gulonate 6-phosphate decarboxylase (KGPDC),[1] is a member of the orotidine 5′-monophosphate decarboxylase (OMPDC) "suprafamily" (*2*−*4*). This suprafamily also includes D-*arabino*-hex-3-ulose 6-phosphate synthase (HPS) that catalyzes the aldol condensation of D-ribulose 5-phosphate with formaldehyde in methylotrophic microbes that "fix" formaldehyde (*5*). The members of this suprafamily share the ubiquitous $(\beta/\alpha)_8$-barrel fold and catalyze mechanistically distinct reactions in different metabolic pathways.

Although the mechanism of the OMPDC-catalyzed reaction remains controversial, it is metal ion-independent and likely proceeds without the formation of an unstable vinyl anion intermediate (*6*, *7*); the value of the pK_a of the C6 proton of UMP (∼34) is too large for the anion to be stable in an aqueous environment (*8*). One proposal for the mechanism is a concerted S_E2 reaction involving simultaneous decarboxylation and protonation at C6 (Figure 1), with the strictly conserved Lys at the end of third β-strand (Lys62 in the structurally characterized OMPDC from *Bacillus subtilis*) functioning as the general acid that delivers a solvent-derived proton to the UMP product (*9*).

† This research was supported by Grant GM-58506 from the National Institutes of Health.

* To whom correspondence should be addressed: Department of Biochemistry, University of Illinois, 600 S. Mathews Ave., Urbana, IL 61801. Phone: (217) 244-7414. Fax: (217) 265-0385. E-mail: j-gerlt@uiuc.edu.

‡ University of Illinois.

§ University of Wisconsin.

[1] Abbreviations: HPS, D-*arabino*-hex-3-ulose 6-phosphate synthase; KGPDC, 3-keto-L-gulonate 6-phosphate decarboxylase; LyxK, 2,3-diketo-L-gulonate kinase; OMPDC, orotidine 5′-monophosphate decarboxylase; XylA, D-xylose isomerase; XylB, D-xylulokinase; YiaK, 2,3-diketo-L-gulonate reductase.

10.1021/bi049741t CCC: $27.50
Published on Web 05/08/2004

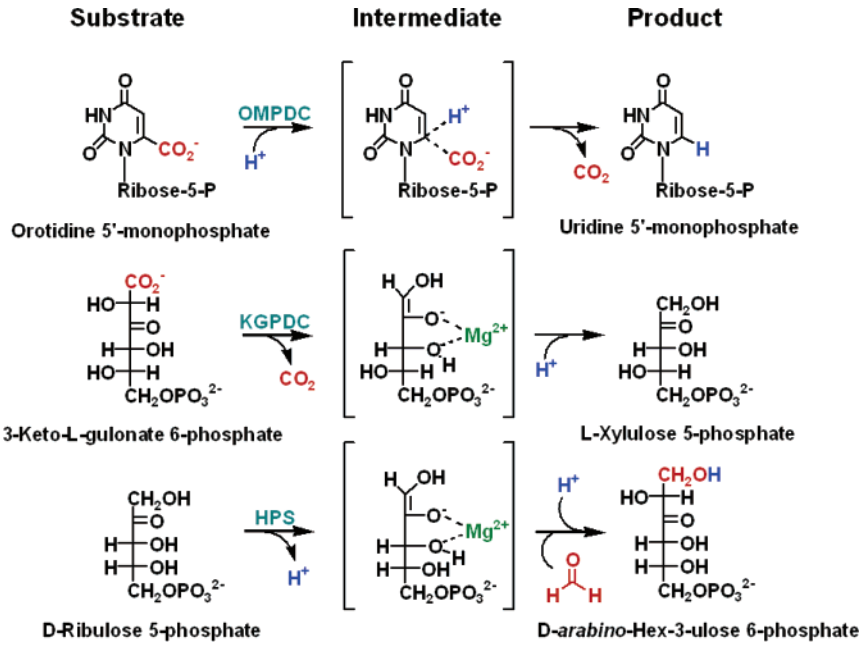

FIGURE 1: Reactions catalyzed by KGPDC, OMPDC, and HPS.

In contrast, the mechanisms of the KGPDC- and HPS-catalyzed reaction can be envisioned to involve enediolate intermediates stabilized by coordination to an essential Mg^{2+} (Figure 1). In the reaction catalyzed by KGPDC, the enediolate intermediate is produced by decarboxylation of the β-keto acid; an active site acid is expected to deliver a proton to the intermediate to generate the L-xylulose 5-phosphate product. In the reaction catalyzed by HPS, an active site base is expected to abstract a C1 proton from the D-ribulose 5-phosphate substrate; formation of a carbon−carbon bond results from attack of this intermediate on the formaldehyde cosubstrate.

The available structures for four OMPDCs [from *E. coli* [Harris, P., Navarro Poulsen, J. C., Jensen, K. F., and Larsen, S. (2000) Structural basis for the catalytic mechanism of a proficient enzyme: orotidine 5′-monophosphate decarboxylase, *Biochemistry 39*, 4217−4224.], *B. subtilis* (*9*), *Methanobacterium thermoautotrophicum* (*10*), and yeast (*11*)] and UlaD, a KGPDC from *E. coli* (*3*), suggest that homologues of residues in the active site of OMPDC have been conscripted to serve different functions in the active site of KGPDC. For example, in the OMPDC from *B. subtilis*, Asp11 at the end of the first β-strand, Lys33 at the end of the second β-strand, and Asp60 at the end of the third β-strand participate in an essential hydrogen bonding network. In KGPDC, the homologous residues, Asp11, Glu33, and Asp62, provide ligands for the essential Mg^{2+}.

On the basis of sequence alignments, the active sites of all KGPDCs and HPSs are predicted to contain conserved homologues of the general acidic Lys residue in the active site of OMPDC (Lys62 in the OMPDC from *B. subtilis*; Figure 2). Indeed, the structure of KGPDC from *E. coli* confirms the expected location of this Lys residue (Lys64) at the end of the third β-strand. Structures are available for four liganded complexes of this KGPDC: the substrate analogue L-gulonate 6-phosphate, the intermediate analogue L-threonohydroxamate 4-phosphate, the product analogue L-xylitol 5-phosphate, and the product L-xylulose 5-phosphate (*3*, *12*). On the basis of these structures, the 3-keto oxygen of the substrate is a ligand of the essential Mg^{2+}, and Lys64 forms a hydrogen bond to the same oxygen to provide additional stabilization of the intermediate. Lys64 is not located in an appropriate position to function as a general acid catalyst that delivers a proton to the enediolate intermediate. However, in the absence of experimental tests of this structure-based mechanism, Lys64 could perform the same function as its homologue in OMPDC, i.e., delivery of a solvent-derived proton to the product, although the reactions involve different intermediates.

On the basis of sequence alignments, the active sites of all KGPDCs and HPSs are predicted to contain a conserved His at the end of the sixth β-strand (His136 in the KGPDC from *E. coli*). Additionally, the active sites of all KGPDCs, but none of the HPSs, are predicted to also contain an Arg residue at the end of the sixth β-strand (Arg139 in the KGPDC from *E. coli*). Perhaps one or both of these residues may function as the general acid in the KGPDC-catalyzed reaction, thereby establishing complete functional divergence of the reactions catalyzed by OMPDC and KGPDC.

Using wild-type KGPDC as well as mutants of several active site residues, we have studied (1) the exchange of the protons of the 1-hydroxymethylene group of the L-xylulose 5-phosphate product with solvent, (2) the stereochemical course of the decarboxylation of 3-keto-L-gulonate 6-phosphate to produce L-xylulose 5-phosphate, and (3) the ability of formaldehyde to intercept the enediolate intermediate in the decarboxylation reaction. Exchange of the product with solvent hydrogen is stereospecific and occurs only when His136 is present, consistent with the essential participation of His136 in this reaction. In contrast, the decarboxylation reaction catalyzed by wild-type KGPDC proceeds with marginal stereoselectivity (favoring inversion of configuration), consistent with the participation of water molecules hydrogen bonded to both His136 and Arg139 as the general acids. The stereochemical course of the decarboxylation can be "tuned" to inversion, retention, or racemization by substitutions for Glu112, His136, and Arg139, presumably by altering the acidities of the associated water molecules.

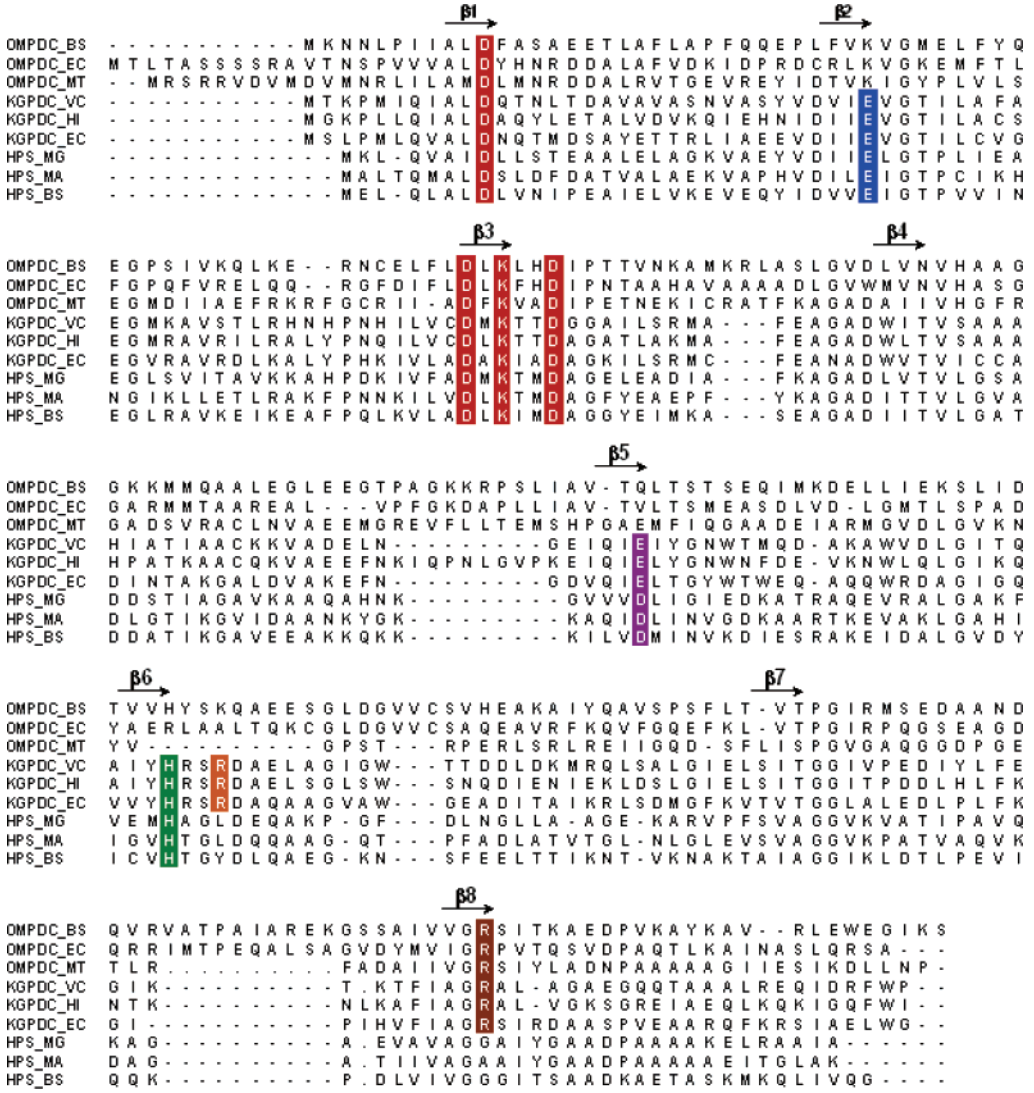

FIGURE 2: Sequence alignment of OMPDCs from *B. subtilis* (OMPDC_BS), *E. coli* (OMPDC_EC), and *M. thermoautotrophicum* (OMPDC_MT), KGPDCs from *Vibrio cholera* (KGPDC_VC), *Haemophilus influenza* (KGPDC_HI), and *E. coli* (KGPDC_EC), and HPSs from *Mycobacterium gastri* (HPS_MG), *Methylomonas aminofaciens* (HPS_MA), and *B. subtilis* (HPS_BS). The strictly conserved Asp11 and residues in the Asp-X-Lys-X-X-Asp motif are highlighted in red. Glu33, the Mg^{2+} binding ligand in KGPDCs and HPSs, is highlighted in blue. The His136−Glu112 dyad in KGPDCs and the His−Asp dyad in HPSs are highlighted in green and magenta, respectively, and the conserved Arg139 is highlighted in orange. A strictly conserved phosphate-binding Arg ligand located at the end of the eighth *β*-strand in KGPDCs and OMPDCs is highlighted in brown. The alignment was produced by the Pileup algorithm of the GCG software package.

Both Lys64 and Asp67 stabilize and restrict the *cis* geometry of the enediolate intermediate but do not directly participate in its protonation. We conclude that, despite homologous active site structures, the reactions catalyzed by OMPDC and KGPDC share no discernible mechanistic relationships, thereby highlighting the opportunistic nature of the likely conscription of an OMPDC progenitor to catalyze the KGPDC reaction.

EXPERIMENTAL PROCEDURES

^{1}H and ^{2}H NMR spectra were recorded using a Varian Unity INOVA 500 MHz NMR spectrometer; ^{13}C and ^{31}P NMR spectra were recorded using a Varian Unity 500 MHz NMR spectrometer. All reagents were the highest quality grade commercially available.

Site-Directed Mutagenesis and Protein Purification. UlaD, the gene encoding one of two KGPDCs in *E. coli*, was previously cloned into a modified pET15-b (Novagen) vector in which the N-terminal His tag contains 10 instead of the usual six His residues (*1*). Site-directed mutants of KGPDC were constructed using the QuikChange kit (Stratagene), verified by sequencing, expressed in the BLR(DE3) *recA*$^{-}$ strain of *E. coli*, and purified as previously described for wild-type KGPDC (*1*).

The presence of contaminating wild-type KGPDC in mutant proteins prepared by this procedure was evaluated as follows. The genes encoding both KGPDCs (*ulaD* in locus AE000491 and *sgbH* in locus AE000435) in strain BW25113 were insertionally inactivated with kanamycin and chloramphenicol resistance markers, respectively (*13*). The D67A, K64R, E112A, and H136A mutants were subcloned into a modified pKK223-3 (Amersham) vector in which the N-terminus contained 10 His residues; the mutants were expressed in the KGPDC-deficient strain, and the kinetic parameters that were obtained were within the error of those measured for proteins isolated from BLR(DE3) (data not shown).

Synthesis of L-Xylulose 5-Phosphate. L-Xylulose was prepared according to the method of Touster et al., with the following modifications. Fifteen grams of L-xylose was refluxed under dry conditions in 150 mL of distilled pyridine for 5 h. Pyridine was removed by evaporation, and unreacted L-xylose was removed by precipitation with ethanol and ether. L-Xylulose 5-phosphate was prepared from L-xylulose and ATP using 2,3-diketo-L-gulonate kinase (LyxK, which utilizes either L-xylulose or 2,3-diketo-L-gulonate as the substrate). The reaction mixture contained 40 mM L-xylulose (10 mmol), 0.76 mM ATP, 13 mM $MgCl_2$, 50 mM K^+HEPES (pH 7.5), 31.7 mM acetyl phosphate (7.9 mmol), 300 units of LyxK, and 400 units of acetate kinase in 250 mL. The reaction mixture was incubated for 3 h at 25 °C. ATP or ADP was removed by treatment with activated charcoal, and the enzymes were removed by filtration through a Biomax-10 (10 000 Da) ultrafiltration membrane (Millipore). L-Xylulose 5-phosphate was purified by elution from a column of DEAE-Sepharose Fast Flow (HCO_3^- form) with a gradient of triethylammonium bicarbonate (pH 8.0). Fractions containing L-xylulose 5-phosphate were pooled, and the triethylammonium bicarbonate was removed by evaporation: ^{1}H NMR (D_2O, 500 MHz) δ 4.36 (q, $J = 19.3$ Hz, 2H), 4.30 (d, $J = 2.2$ Hz, 1H), 3.95 (dt, $J = 2.2$, 6.5 Hz, 1H), 3.60 (m, 2H); ^{13}C NMR (D_2O, 500 MHz) δ 181.0, 73.0, 71.5, 68.5, 67.0.

Synthesis of D-[1R-^{2}H]Xylulose 5-Phosphate. D-[1*R*-^{2}H]-Xylulose 5-phosphate was prepared from commercially available D-[2-^{2}H]xylose (Omicron) using D-xylose isomerase (XylA) and D-xylulokinase (XylB). The reaction mixture contained 44 mM D-[2-^{2}H]xylose (2.2 mmol), 0.13 mM ATP, 30 mM $MgCl_2$, 50 mM maleate (pH 7.0), 52 mM acetyl phosphate (2.6 mmol), 300 units of acetate kinase, 200 units of XylA, and 200 units of XylB in 50 mL. The reaction mixture was incubated for 3 h at 25 °C. D-[1*R*-^{2}H]Xylulose 5-phosphate was purified as previously described for L-xylulose 5-phosphate. The genes encoding XylA and XylB were cloned from genomic DNA isolated from *E. coli* strain MG 1655 and expressed using a modified pET15-b vector encoding an N-terminal His tag with 10 His residues. The proteins were expressed in *E. coli* strain BL21(DE3) and purified as described for KGPDC.

KGPDC-Catalyzed Exchange of the Protons of the 1-Hydroxymethylene Group of L-Xylulose 5-Phosphate. L-Xylulose 5-phosphate was incubated with KGPDC in D_2O buffer at 20 °C, and ^{1}H NMR spectra were recorded as a function of time. A typical reaction mixture contained 20 mM L-xylulose 5-phosphate, 50 mM K^+HEPES (pD 7.5), 10 mM $MgCl_2$, and 5 μM wild-type KGPDC (or increased amounts of mutant enzymes). The rate of exchange (k_{exc}) of the protons of the 1-hydroxymethylene group by wild-type KGPDC was calculated from eq 1, which takes into account the total amount of L-xylulose 5-phosphate bound at any time.

$$k_{exc} = k_{obs}[LX5P]_T/[LX5P]_B \quad (1)$$

where k_{obs} is the observed first-order rate constant, $[LX5P]_T$ is the total L-xylulose 5-phosphate concentration, and $[LX5P]_B$ is the concentration of bound L-xylulose 5-phosphate. Because the concentration of L-xylulose 5-phosphate (20 mM) was significantly higher than the enzyme concentration (5 μM), the concentration of bound L-xylulose 5-phosphate ($[LX5P]_B$) was equal to the enzyme concentration.

Stereochemical Course of 3-Keto-L-gulonate 6-Phosphate Decarboxylation. 3-Keto-L-gulonate 6-phosphate was generated *in situ* and decarboxylated in a D_2O-containing buffer at 20 °C, with ^{1}H NMR spectra recorded as a function of time after initiation of the reaction. We observed the immediate production of 3-keto-L-gulonate 6-phosphate that underwent enzyme-catalyzed decarboxylation; however, in the absence of KGPDC, the substrate slowly epimerizes at C2 to 3-keto-L-idonate 6-phosphate (not shown). To minimize this competing reaction, KGPDC was present when the substrate was generated. A typical reaction mixture contained 20 mM 2,3-diketo-L-gulonate, 50 mM K^+HEPES (pD 7.5), 10 mM $MgCl_2$, 0.25 mM ATP, 0.25 mM NADH, 20 mM sodium formate, 20 mM acetyl phosphate, 150 units of 2,3-diketo-L-gulonate reductase (YiaK), 50 units of LyxK, 10 units of formate dehydrogenase, 20 units of acetate kinase, and 5 μM wild-type KGPDC (or increased amounts of mutant enzymes). All enzymes were exchanged into D_2O buffer [50 mM K^+HEPES (pD 7.5)] using an Amicon (10 000 Da) stirred ultrafiltration cell.

Formaldehyde as an Alternate Electrophile in Decarboxylation. 3-Keto-L-gulonate 6-phosphate was generated *in situ* as previously described and decarboxylated in a D_2O-containing buffer at 20 °C in the presence of formaldehyde, with ^{1}H NMR spectra recorded as a function of time after initiation of the reaction. A typical reaction mixture contained all previously described components with the addition of 3.75−37.5 mM formaldehyde (generated from a 1 M stock of paraformaldehyde in D_2O).

Synthesis of L-[1-$^2H_2$]Xylulose 5-Phosphate. L-[1-$^2H_2$]-Xylulose 5-phosphate was prepared by decarboxylation of 3-keto-L-gulonate 6-phosphate in D_2O buffer using the D67A mutant. The reaction mixture contained 20 mM 2,3-diketo-L-gulonate (0.16 mmol), 0.25 mM ATP, 0.25 mM NADH, 10 mM $MgCl_2$, 50 mM K^+HEPES (pD 7.5), 20 mM acetyl phosphate (0.16 mmol), 20 mM sodium formate (0.16 mmol), 1500 units of YiaK, 500 units of LyxK, 100 units of formate dehydrogenase, 200 units of acetate kinase, and 1000 units of D67A in 8 mL. The reaction mixture was incubated for 20 min at 25 °C, and enzymes were removed by filtering the mixture with a Biomax-10 (10 000 Da) ultrafiltration membrane (Millipore). Unincorporated deuterium was removed from the solution containing L-[1-$^2H_2$]xylulose 5-phosphate by repeated lyophilization from deuterium-depleted H_2O: ^{2}H NMR (H_2O, 500 MHz) δ 4.45 and 4.35 for *pro*-1*S* and *pro*-1*R* deuteria, respectively.

Deuterium NMR Studies of KGPDC-Catalyzed Exchange of the Protons of the 1-Hydroxymethylene Group of L-[1-$^2H_2$]Xylulose 5-Phosphate. L-[1-$^2H_2$]Xylulose 5-phosphate was incubated with 5 μM wild-type KGPDC or increased amounts of mutants in deuterium-depleted buffer for 210 min at 20 °C, and ^{2}H NMR spectra were recorded. A typical reaction mixture contained 20 mM L-[1-$^2H_2$]xylulose 5-phosphate, 50 mM K^+HEPES (pH 7.5), 10 mM $MgCl_2$, and enzyme. All enzymes were exchanged into deuterium-depleted buffer [50 mM K^+HEPES (pH 7.5)] using an Amicon (10 000 Da) stirred ultrafiltration cell.

Deuterium NMR Studies of the Stereochemical Course of 3-Keto-L-gulonate 6-Phosphate Decarboxylation. [2-^{2}H]-3-Keto-L-gulonate 6-phosphate was generated *in situ* and

decarboxylated in deuterium-depleted (2−3 ppm deuterium) buffer at 20 °C, and ^{2}H NMR spectra were recorded as a function of time after initiation of the reaction. A typical reaction mixture contained 20 mM 2,3-diketo-L-gulonate, 50 mM K^+HEPES (pH 7.5), 10 mM $MgCl_2$, 0.25 mM ATP, 0.25 mM NADH, 20 mM sodium [^{2}H]formate (≥99 at. % ^{2}H, Isotec), 20 mM acetyl phosphate, 150 units of YiaK, 50 units of LyxK, 10 units of formate dehydrogenase, 20 units of acetate kinase, and KGPDC in deuterium-depleted (2−3 ppm) H_2O (Cambridge Isotope Laboratories). All enzymes were exchanged into deuterium-depleted buffer [50 mM K^+-HEPES (pH 7.5)] using an Amicon (10 000 Da) stirred ultrafiltration cell.

Kinetic Assay of KGPDC. Proteins were assayed for KGPDC activity as previously described (*1*). Briefly, a stock solution of 3-keto-L-gulonate 6-phosphate was generated *in situ* by incubating 2,3-diketo-L-gulonate (3.0−6.0 mM), 10 mM $MgCl_2$, ATP (6−10 mM), 80 units/mL YiaK, 80 units/mL LyxK, and 1 equiv of NADH for 10 min at 25 °C. The assay mixtures (1 mL) contained 3-keto-L-gulonate 6-phosphate (0.078−5.0 mM), 50 mM K^+HEPES (pH 7.5), and 10 mM $MgCl_2$. After incubation at 25 °C for sufficient time to convert ≤10% of the substrate to product, the enzymes were removed by centrifugation through a Biomax-10 (10 000 Da) Millipore centrifugal device. The L-xylulose 5-phosphate product was dephosphorylated by incubation with calf intestinal alkaline phosphatase (CIAP) at 37 °C for 5 min. CIAP was precipitated from the mixture by addition of 300 μL each of a 5% solution of $ZnSO_4 \cdot 7H_2O$ and 0.15 M $Ba(OH)_2$. The supernatant was assayed for L-xylulose by reaction with L-cysteine and carbazole and by measuring the absorbance at 540 nm.

RESULTS AND DISCUSSION

In our initial report about the structure of the Mg^{2+}-requiring KGPDC (*3*), we suggested a mechanism in which the 2-OH group and 3-keto group of the substrate are liganded to the Mg^{2+}; decarboxylation would yield a *cis*-1,2-enediolate with the 1- and 2-oxygens liganded to the Mg^{2+} to provide essential stabilization. However, as a result of our more recent structural studies with analogues of the substrate (L-gulonate 6-phosphate), enediolate intermediate (L-threonohydroxamate 4-phosphate), and product (L-xylitol 5-phosphate) as well as with the actual L-xylulose 5-phosphate product, we now hypothesize a mechanism in which the 3-keto group and the 4-OH group of the substrate are liganded to the Mg^{2+} and the 2-OH group is hydrogen-bonded to Asp67 from the adjacent polypeptide in the dimer (*12*).

The structure of the complex of KGPDC with L-threonohydroxamate 4-phosphate, the analogue of the *cis*-1,2-enediolate, is shown in Figure 3. In the mechanism that is consistent with this structure, the *cis*-1,2-enediolate intermediate is stabilized by coordination of the 2-oxygen to the Mg^{2+} and hydrogen bonding of the 1-oxygen with Asp67. Lys64 also interacts with both the 1- and 2-oxygens of the intermediate to provide additional stabilization. The direct interactions of both Lys64 and Asp67 with the intermediate and the indirect interactions of Asp11 and Glu33 via the liganded Mg^{2+} would require that a functional group not present in OMPDC protonate the enediolate intermediate to form the L-xylulose 5-phosphate product. On the basis of the structures of the various complexes, we hypothesized that Glu112, His136, or their hydrogen-bonded dyad functions as the general acid catalyst (*12*).

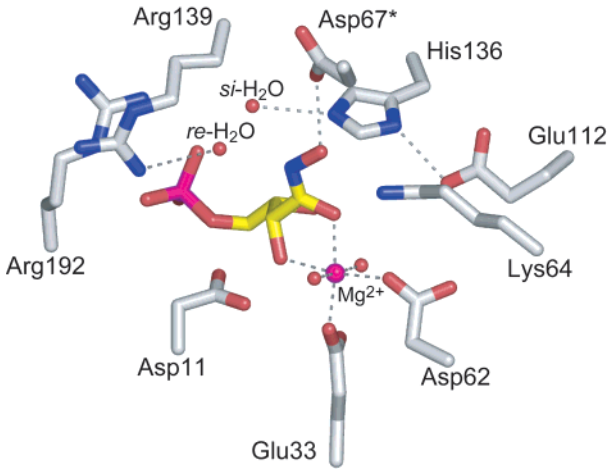

FIGURE 3: Structure of the active site of wild-type KGPDC complexed with L-threonohydroxamate 4-phosphate, an analogue of the *cis*-1,2-enediolate intermediate, showing the locations of the water molecules located on the *re*- and *si*-faces of the intermediate.

Table 1: Kinetic Parameters of KGPDC

	k_{cat} (s^{-1})	K_M (M)	k_{cat}/K_M (M^{-1} s^{-1})
wild type	51 ± 2	(6.7 ± 0.2) × 10^{-4}	7.7 × 10^4
E33K	∼0	−	∼0
K64R	17 ± 1	(3.0 ± 0.1) × 10^{-4}	5.7 × 10^4
K64A	8.3 ± 0.1	(5.1 ± 0.2) × 10^{-4}	1.6 × 10^4
D67N	1.1 ± 0.1	(4.1 ± 0.1) × 10^{-4}	2.7 × 10^3
D67A	2.4 ± 0.2	(5.0 ± 0.2) × 10^{-4}	4.8 × 10^3
E112Q	4.0 ± 0.3	(3.1 ± 0.1) × 10^{-4}	1.3 × 10^4
E112A	0.3 ± 0.02	(3.4 ± 0.1) × 10^{-4}	8.8 × 10^2
H136N	4.3 ± 0.4	(3.7 ± 0.1) × 10^{-4}	1.3 × 10^4
H136Q	1.4 ± 0.06	(5.2 ± 0.3) × 10^{-4}	2.7 × 10^3
H136A	2.4 ± 0.1	(7.0 ± 0.2) × 10^{-4}	3.4 × 10^3
R139V	8.9 ± 0.2	(3.6 ± 0.3) × 10^{-4}	2.5 × 10^4
D67N/H136A	1.3 ± 0.1	(3.0 ± 0.09) × 10^{-4}	4.3 × 10^3
D67A/H136A	0.19 ± 0.008	(2.7 ± 0.05) × 10^{-4}	7.0 × 10^2
K64R/H136A	4.2 ± 0.16	(4.4 ± 0.5) × 10^{-4}	9.5 × 10^3
K64A/H136A	0.75 ± 0.05	(5.8 ± 0.1) × 10^{-4}	1.3 × 10^3
E112Q/H136A	0.23 ± 0.01	(1.5 ± 0.03) × 10^{-4}	1.5 × 10^3
E112A/H136A	0.45 ± 0.03	(6.5 ± 0.6) × 10^{-4}	6.9 × 10^2
K64A/R139V	1.2 ± 0.1	(9.0 ± 1.0) × 10^{-4}	1.3 × 10^3
H136A/R139V	9.2 ± 0.4	(1.4 ± 0.3) × 10^{-3}	6.6 × 10^3
K64A/E112Q/H136A	2.9 ± 0.2	(5.5 ± 0.9) × 10^{-4}	5.3 × 10^3
E112Q/H136A/R139V	0.2 ± 0.015	(2.2 ± 0.2) × 10^{-4}	9.1 × 10^2
E112A/H136A/R139V	0.21 ± 0.01	(7.7 ± 0.6) × 10^{-4}	2.7 × 10^2
K64A/E112A/H136A/R139V	0.26 ± 0.02	(1.4 ± 0.2) × 10^{-3}	1.9 × 10^2

Glu112 and His136 are expected to be located on the *si*-face of C1 of the intermediate (Figure 3). The configuration of C2 of the 3-keto-L-gulonate 6-phosphate substrate is consistent with carbon dioxide departing from the *re*-face of C1 of the resulting enediolate intermediate. Therefore, if Glu112 and/or His136 were the acid, the KGPDC-catalyzed reaction would proceed with inversion of configuration. We now report experiments that examine these predictions.

Kinetic Parameters of Active Site Mutants. Single and multiple mutants involving several active site residues were constructed; the identities of the various mutants and the values of their kinetic constants are summarized in Table 1.

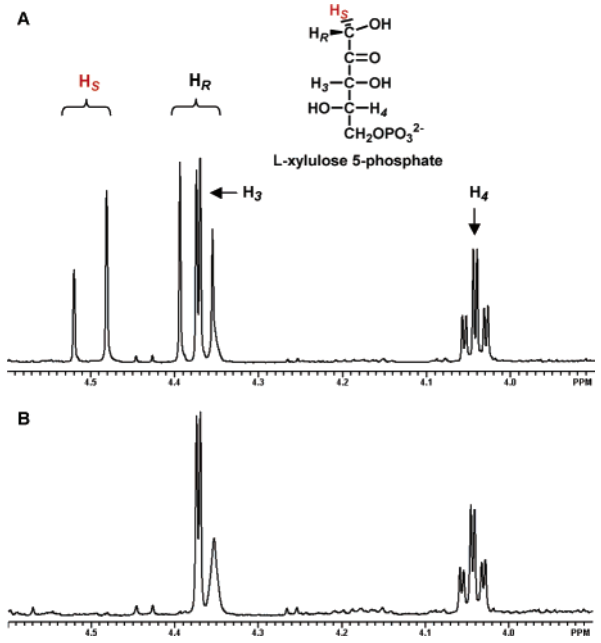

FIGURE 4: (A) ^{1}H NMR spectrum of L-xylulose 5-phosphate, showing the assignments of the 1-hydroxymethylene protons. (B) Representative spectrum of 20 mM L-xylulose 5-phosphate after incubation with wild-type KGPDC or the various mutants of Lys64, Asp67, Glu112, and Arg139 listed in Table 1.

Enzymatic decarboxylation of β-keto acids can occur via two mechanisms. (1) An active site lysine stabilizes the electron-rich intermediate derived from decarboxylation as a ketimine, as in the case of acetoacetate decarboxylase (*14*, *15*). (2) A divalent metal ion stabilizes an enolate intermediate by direct coordination, as in the case of class II aldolases (*16*, *17*). The reaction catalyzed by KGPDC is dependent on the presence of Mg^{2+} (*1*). However, the presence of Lys64 suggests that a Schiff base mechanism could be possible. That the value of k_{cat} for the K64A mutant is 20% of that of the wild type eliminates this mechanistic possibility.

Surprisingly, single mutants of Lys64, Asp67, Glu112, His136, and Arg139, candidates for substrate binding and/or catalysis of proton transfers based on the available structural information (*12*), retain substantial activity.

Exchange of the Protons of the 1-Hydroxymethylene Group of L-Xylulose 5-Phosphate with Solvent. The ^{1}H NMR spectrum of L-xylulose 5-phosphate includes an AB quartet associated with the geminal protons of the 1-hydroxymethylene group. A sample of D-[1*R*-^{2}H]xylulose 5-phosphate was prepared from D-[2-^{2}H]xylose by the coupled action of D-xylose isomerase (XylA) and D-xylulose kinase (XylB); Rose (*18*) reported that the hydride transfer reaction catalyzed by XylA is accompanied by migration of the 2-hydrogen of D-xylose to the 1*R* position of D-xylulose. The downfield resonance of the AB quartet was selectively depleted in the spectrum of the deuterated D-xylulose 5-phosphate. Hence, the downfield resonance of the AB quartet in the enantiomeric L-xylulose 5-phosphate is associated with the *pro*-1*S* hydrogen (Figure 4A).

We investigated whether KGPDC can catalyze exchange of one or both of the prochiral 1-hydroxymethylene protons of the L-xylulose 5-phosphate product with solvent. Wild-type KGPDC catalyzes a stereospecific exchange in which L-[1*S*-^{2}H]xylulose 5-phosphate is formed (Figure 4B). The value of the rate constant for exchange of the *pro*-1*S* proton (k_{exc}) is 0.96 $\pm$ 0.03 s^{-1}, 2% of the value of k_{cat} measured for decarboxylation (Table 1). This difference in rate constants suggests that (1) the conjugate acid of the base that catalyzes exchange is monoprotic and not readily accessible to solvent and/or (2) the functional group that catalyzes the exchange reaction is significantly protonated at pH 7.5, as might be expected if this group were the general acid in the decarboxylation reaction.

The ability of KGPDC to catalyze stereospecific exchange of a proton of the L-xylulose 5-phosphate product is persuasive evidence for the occurrence of an enediolate intermediate.

Exchange of the Protons of the 1-Hydroxymethylene Group of the L-Xylulose 5-Phosphate Product with Solvent Catalyzed by Mutant Enzymes. We also studied the ability of mutants to catalyze exchange of the 1-hydroxymethylene protons of the L-xylulose 5-phosphate product with solvent. For experimental convenience, we increased the amounts of enzyme in inverse proportion to the effect of the substitutions on activity to facilitate data collection. Single substitutions for Lys64, Asp67, Glu112, and Arg139 catalyzed stereospecific exchange of the *pro*-1*S* hydrogen, as was observed for the wild-type enzyme (Figure 4B). In contrast, single substitutions for His136 as well as all multiple mutants that contained the H136A substitution were unable to catalyze the exchange reaction (data not shown). This observation is consistent with His136 catalyzing stereospecific exchange of the protons of the 1-hydroxymethylene group of the product with solvent. The expected corollary is that His136 catalyzes delivery of a proton to the enediolate in the decarboxylation reaction.

Stereochemical Course of 3-Keto-L-gulonate 6-Phosphate Decarboxylation. We then determined the stereochemical course of the decarboxylation reaction catalyzed by KGPDC so that we could determine the relative orientation of the carboxylate group that departs as CO_2 and the general acid that delivers a solvent-derived proton to the stabilized enediolate intermediate to yield the product. This requires both configurational assignment of the substrate as well as chemical shift assignments for the diastereotopic prochiral protons of the hydroxymethylene group of the L-xylulose 5-phosphate product.

The substrate used in our experiments is generated *in situ* from 2,3-diketo-L-gulonate using NADH, 2,3-diketo-L-gulonate reductase (YiaK), ATP, and 3-keto-L-gulonate kinase (LyxK). We determined that 2,3-diketo-L-gulonate is reduced by YiaK to yield 3-keto-L-gulonate, not the 2-epimeric 3-keto-L-idonate; this was accomplished by enzymatically reducing 2,3-diketo-L-gulonate with YiaK followed by chemical reduction of the resulting 3-ketoacid with $NaBH_4$. The ^{1}H NMR spectrum of this sample was identical to that of a mixture of L-gulonate and L-galactonate rather than a mixture of L-talonate and L-idonate (data not shown), thereby establishing the identity of the substrate as 3-keto-L-gulonate 6-phosphate.

When 3-keto-L-gulonate 6-phosphate is decarboxylated by wild-type KGPDC in a D_2O buffer, both L-[1*S*-^{2}H]- and L-[1*R*-^{2}H]xylulose 5-phosphate are produced, the former being favored by a modest 2:1 ratio (Figure 5A). The stereochemical course of decarboxylation to yield the more abundant L-[1*S*-^{2}H]xylulose 5-phosphate is inversion of configuration, as predicted from the observed stereospeci-

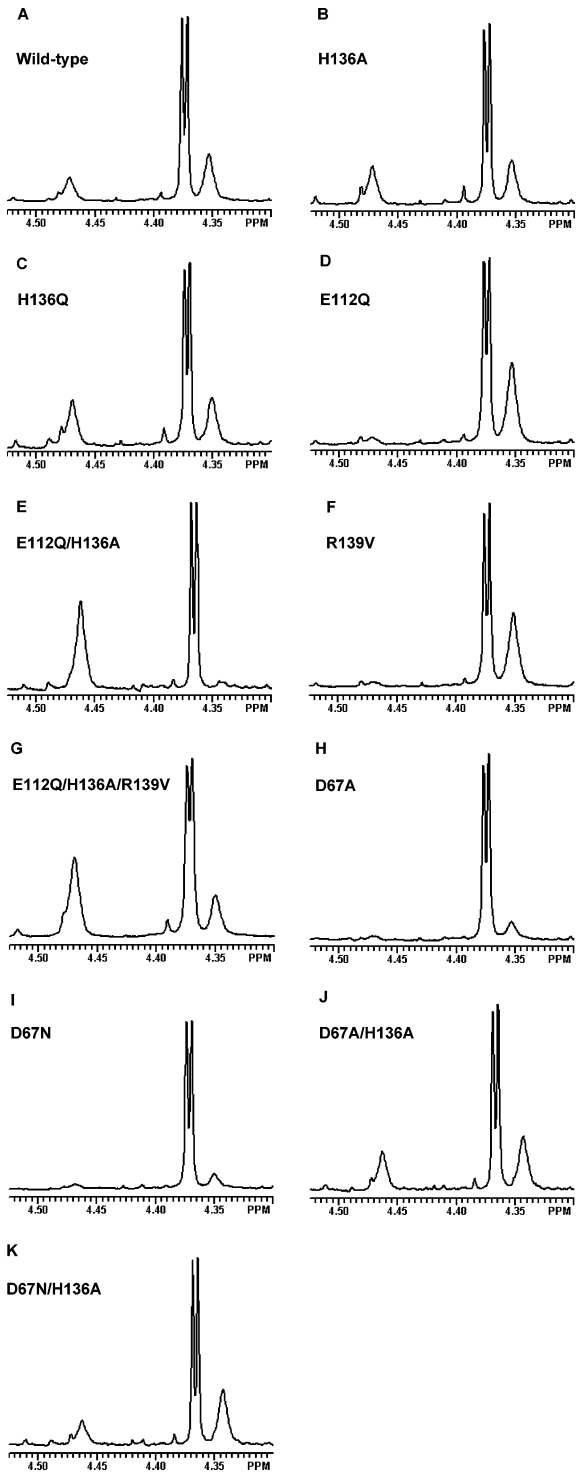

FIGURE 5: Partial ^{1}H NMR spectra of L-xylulose 5-phosphate obtained from the decarboxylation of 3-keto-L-gulonate 6-phosphate in D_2O using (A) wild-type KGPDC, (B) H136A, (C) H136Q, (D) E112Q, (E) E112Q/H136A, (F) R139V, (G) E112Q/H136A/R139V, (H) D67A, (I) D67N, (J) D67A/H136A, and (K) D67N/H136A.

ficity of exchange of the *pro*-1*S* hydrogen of L-xylulose 5-phosphate with solvent hydrogen; the less abundant L-[1*R*-^{2}H]xylulose 5-phosphate is formed with an unanticipated retention of configuration.

The reactions catalyzed by KGPDC and other β-ketoacid decarboxylases yield achiral products [either a methylene or a methyl group is produced by protonation of the en(edi)-olate/enamine intermediate], so no evolutionary pressure can be used to enforce a defined stereochemical course. Nevertheless, the lack of stereospecificity in the KGPDC-catalyzed β-ketoacid decarboxylation reaction is unusual, but not unprecedented; the reactions catalyzed by some β-ketoacid decarboxylases proceed with retention of configuration (isocitrate dehydrogenase and malic enzyme), and others proceed with inversion of configuration (phosphogluconate dehydrogenase, UDP-glucuronate dehydrogenase, acetolactate dehydrogenase, and oxaloacetate decarboxylase) (*19*). Only the reaction catalyzed by acetoacetate decarboxylase proceeds with racemization (*20*). In the case of the KGPDC-catalyzed reaction, the lack of stereospecificity in protonation of the *cis*-enediolate intermediate may be a consequence of the functional divergence from an active site that catalyzes the achiral OMPDC reaction.

Two explanations are possible for the unexpected lack of stereospecificity.

(1) Protonation of the intermediate to yield product occurs by two competing pathways, one in which a proton is delivered to the *si*-face of C1 of the *cis*-enediolate intermediate to yield L-[1*S*-^{2}H]xylulose 5-phosphate and the second in which a proton is delivered to the *re*-face to yield L-[1*R*-^{2}H]xylulose 5-phosphate. Glu112 and His136 are both positioned on the *si*-face, making one or both of these candidates for the *si*-face specific catalyst. However, the available structures also reveal the presence of a water molecule hydrogen bonded to His136 in a position more appropriate for delivery of a proton to the *si*-face (Figure 3). No potential amino acid general acidic catalyst is located on the *re*-face of C1 of the intermediate, although the available structures reveal the presence of one or two water molecules proximal to Arg139 that are in positions that are appropriate for delivery of a proton to the *re*-face (Figure 3).[2]

(2) Both *cis*- and *trans*-enediolate intermediates can exist in the active site, with the consequence that the same protein functional group delivers a proton to the *si*-face of C1 of the *cis*-enediolate and the *re*-face of C1 of the *trans*-enediolate, resulting in the observed mixture of L-[1*S*-^{2}H]- and L-[1*R*-^{2}H]xylulose 5-phosphates.

The experiments described in the remainder of this paper explore the validity of these explanations.

Stereochemical Course of the Decarboxylation Reactions Catalyzed by Active Site Mutants. We examined the stereochemical courses of the decarboxylation reactions catalyzed by mutants using increased amounts of the proteins to allow the rate of the decarboxylation reaction to exceed that of the competing nonenzymatic 2-epimerization of the 3-keto-L-gulonate 6-phosphate substrate to 3-keto-L-idonate 6-phosphate. We sought explanations for (1) the modest stereospecificity with respect to delivery of a solvent-derived proton in the decarboxylation reaction catalyzed by wild-type KGPDC and (2) the surprisingly small effects of mutations

[2] That the enzyme catalyzes stereospecific exchange of solvent-derived hydrogen from the L-xylulose 5-phosphate product via a stabilized 1,2-enediolate intermediate but stereorandom delivery of solvent-derived hydrogen to a stabilized 1,2-enediolate intermediate generated by decarboxylation need not violate the principle of microscopic reversibility. The intermediates are generated by different mechanisms in the two processes. Indeed, the much slower rate of the exchange reaction relative to the overall decarboxylation reaction may be explained by different active site conformations or protonation states for the active site residues in the two processes.

on the values of the kinetic constants for decarboxylation. The ^{1}H NMR spectra of the L-xylulose 5-phosphate products for the reactions catalyzed by several of the mutants are shown in Figure 5.

Several pertinent observations were made.

(1) Substitutions for Glu112 and His136 that are located on the *si*-face of C1 of the enediolate intermediate produce a spectrum of effects. First, like wild-type KGPDC, substitutions for His136 (H136A/N/Q) produce nearly stereorandom formation of mixture of L-[1*S*-^{2}H]- and L-[1*R*-^{2}H]xylulose 5-phosphates, despite our observation that His136 is required for stereospecific exchange of the *pro*-1*S* hydrogen of L-xylulose 5-phosphate (Figure 5B,C). Second, E112Q shows *stereospecific* formation of L-[1*S*-^{2}H]xylulose 5-phosphate, an *enhancement* of the facial specificity for protonation of the enediolate intermediate observed for wild-type KGPDC (Figure 5D); this decarboxylation reaction proceeds with inversion of configuration. Third, the E112Q/H136A double mutant shows *stereospecific* formation of L-[1*R*-^{2}H]xylulose 5-phosphate, a *reversal* of that observed for wild-type KGPDC (Figure 5E); this decarboxylation reaction proceeds with retention of configuration.

We propose that the changes in the facial selectivity for protonation of the enediolate intermediate (and, therefore, the stereochemical course of the reaction) cannot be explained by alternate or competing protein-derived acid catalysts located on opposite faces of the intermediate. Instead, we propose that the acidities of the water molecules located on opposite faces of the enediolate intermediate substitutions are controlled by the electrostatic environment within the active site. For example, the His136−Glu112 dyad may stabilize the protonated state of His136 that is hydrogen bonded to a water molecule, thereby enhancing the acidity of hydrogen-bonded water. When Glu112 is "removed" in the E112Q mutant, the density of the positive charge located on His136 will be increased, further enhancing the acidity of the associated water molecule and transfer of a proton to the *si*-face of C1 of the enediolate intermediate. Consistent with this scenario, in the E112Q/H136A double mutant, the water molecule located on the *si*-face will be deactivated for proton delivery, thereby allowing the observed dominance of proton transfer to the *re*-face.

The observed stereorandom protonation of the enediolate intermediate in the decarboxylation reactions catalyzed by the various single substitutions for His136 may be explained by the ability of the conjugate acid of Glu112 to activate an associated water molecule for delivery of a proton to the *si*-face of C1 of the intermediate so that protonation on this face remains competitive with protonation on the *re*-face.[3]

(2) The R139V substitution results in stereospecific production of L-[1*S*-^{2}H]xylulose 5-phosphate (Figure 5F). This suggests a role for Arg139 in delivering a proton to the *re*-face of the enediolate intermediate. In the structures of wild-type KGPDC complexed with both the intermediate analogue L-threonohydroxamate 4-phosphate and the L-xylulose 5-phosphate product, a water molecule on the *re*-face of C1 is located, on average, 2.7 Å from the guanidinium group of Arg139, suggesting that the acidity of this water, like that located on the *si*-face, is altered by the proximal cationic functional group.

(3) The E112Q/H136A/R139V triple mutant, in which all three of the protein functional groups implicated in modulating the acidities of active site water molecules are "neutralized", produces stereorandom production of L-[1*S*-^{2}H]- and L-[1*R*-^{2}H]xylulose 5-phosphates (Figure 5G). This is consistent with either uncatalyzed stereorandom protonation from the active site water molecules or release of the enediolate intermediate to bulk solvent for protonation.

The decreased rate of product formation that accompanies all of the mutants described in this section (Table 1) may be explained by the expectation that removal of cationic residues will not only decrease the acidities of active site water molecules but also destabilize the proximal anionic enediolate intermediate.

(4) The decarboxylation reactions catalyzed by D67A and D67N are accompanied by nearly complete dideuteration of the hydroxymethyl group of the product (Figure 5H,I), requiring delivery of deuterium to the intermediate as well as subsequent exchange of the substrate-derived hydrogen in the product, presumably by His136 (*vide infra*). This supports the proposal that Asp67 "grips" the enediolate intermediate via its 1-oxygen; additional experimental results that confirm this supposition will be presented subsequently.

In the D67A/H136A and D67N/H136A double mutants, the solvent exchange reactions observed for D67A and D67N are eliminated, although preferential formation of L-[1*S*-^{2}H]-xylulose 5-phosphate is still observed (Figure 5J,K). These observations are consistent with the previously established role of His136 in catalyzing exchange of the L-xylulose 5-phosphate product with solvent.

Taken together, the modest impact of the various mutations on catalytic activity and the remarkable ability to alter the facial selectivity of delivery of a proton to the *cis*-enediolate intermediate provide persuasive evidence that the protonation of the intermediate is not the result of direct transfer of protons from amino acid functional groups. Instead, we propose that protonation of the intermediate results from electrostatic enhancement of the acidities of water molecules by spatially proximal active site residues: the Glu112−His136 dyad enhances the acidity of a water molecule located on the *si*-face of C1, and Arg139 enhances the acidity of a water molecule located on the *re*-face.

Facial Access of the Enediolate Intermediate to Formaldehyde. On the basis of the structure of the complexes of the wild-type KGPDC with L-threonohydroxamate intermediate analogue and the L-xylulose 5-phosphate product, we proposed that Asp67 forms a hydrogen bond to the 2-OH group of the 3-keto-L-gulonate 6-phosphate substrate and, after decarboxylation, the 1-oxygen of the enediolate intermediate and the 1-OH group of the product. In this context, the observation that the decarboxylation reactions catalyzed by the D67N and D67A mutants are accompanied by exchange of the substrate-derived proton may be explained by a relaxation of these conformational "requirements", with decarboxylation yielding a *trans*-enediolate intermediate that is protonated on either the *re*- or *si*-face of C1 and then, with the assistance of the conjugate base of His136, undergoes exchange with solvent. When the H136A substitu-

[3] In the available liganded structures of wild-type KGPDC (*3*), neither the distance between His136 and the enediolate intermediate nor the orientation of His136 with respect to C1 of the intermediate is appropriate for direct delivery of a proton to the intermediate. Instead, as discussed herein, we hypothesize that the water molecule hydrogen-bonded to His136 delivers a proton to the *si*-face of the intermediate.

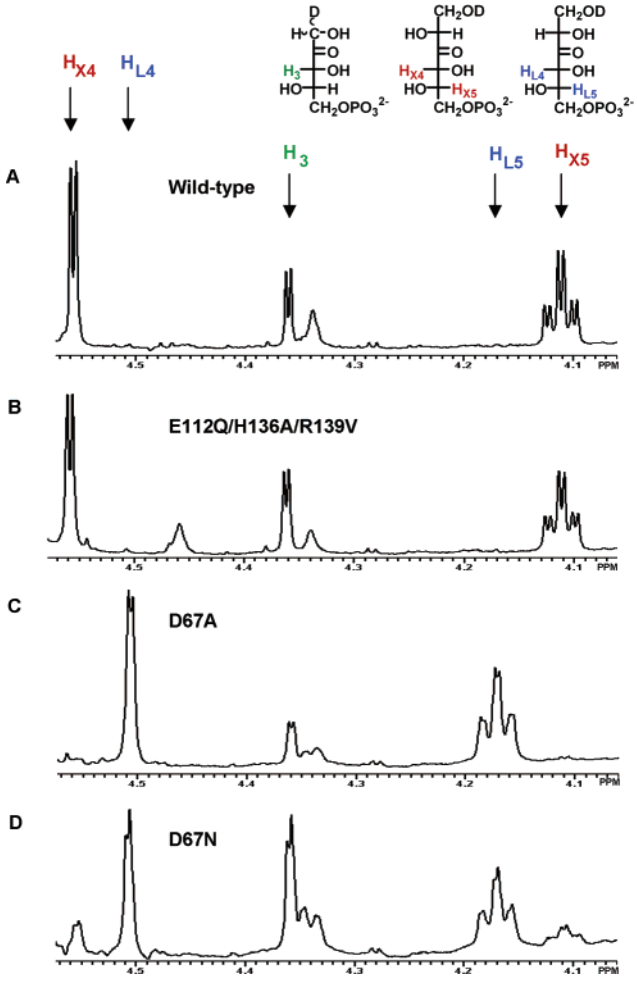

FIGURE 6: Partial ^{1}H NMR spectra of the products obtained from the decarboxylation of 3-keto-L-gulonate 6-phosphate in D_2O in the presence of formaldehyde using (A) wild-type KGPDC, (B) E112Q/H136A/R139V, (C) D67A, and (D) D67N.

tion is also present, the decarboxylation reaction is accompanied by stereorandom incorporation of solvent hydrogen. Therefore, we sought independent evidence for the formation of *trans*-enediolate intermediates in the decarboxylation reactions catalyzed by D67A and D67N.

HPS that catalyzes the aldol condensation of D-ribulose 5-phosphate with formaldehyde is a homologue of KGPDC. We have determined that KGPDC is catalytically promiscuous; in the presence of 18.75 mM formaldehyde, the KGPDC-catalyzed decarboxylation of 3-keto-L-gulonate 6-phosphate produces both L-xylulose 5-phosphate and one diastereomer (at C2) of L-hex-3-ulose 6-phosphate in a 1:3 ratio (Figure 6A); i.e., remarkably, formaldehyde can be a better electrophile than a solvent-derived proton for the enediolate intermediate.

The same diastereomer of L-hex-3-ulose 6-phosphate is produced by most mutants, including the E112Q mutant that yields L-[1*S*-^{2}H]xylulose 5-phosphate, the E112Q/H136A mutant that yields L-[1*R*-^{2}H]xylulose 5-phosphate, the R139V mutant that also yields L-[1*S*-^{2}H]xylulose 5-phosphate, and the E112Q/H136A/R139V mutant that yields a mixture of L-[1*S*-^{2}H]- and L-[1*R*-^{2}H]xylulose 5-phosphates (Figure 6B). Thus, irrespective of the facial selectivity for protonation of the enediolate intermediate, formaldehyde intercepts the enediolate intermediate from only a single face, presumably that which is most accessible to solvent.

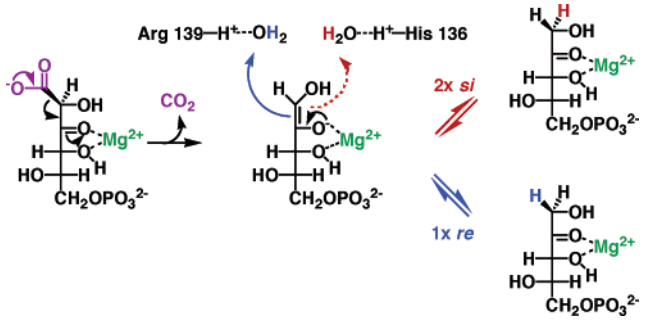

FIGURE 7: Proposed mechanism for KGPDC-catalyzed decarboxylation of 3-keto-L-gulonate 6-phosphate.

In contrast, the D67A mutant yields the other 2-diastereomer of L-hex-3-ulose 6-phosphate (Figure 6C), and the D67N mutant yields a mixture of both diastereomers (Figure 6D). The altered stereochemical course for the aldol condensation with formaldehyde is most readily explained by the formation of a *trans*-enediolate intermediate in the reactions catalyzed by the D67A and D67N mutants, with the existence of this intermediate also being consistent with the observed incorporation of solvent-derived hydrogen as well as exchange of the substrate-derived hydrogen in the decarboxylation reaction.

That the various mutants involving Glu112, His136, and Arg139 yield the same aldol product provides persuasive support for our conclusion that the differing stereochemical courses for the decarboxylation reactions catalyzed by the same mutants result from protonation from opposite faces of a *cis*-enediolate intermediate (Figure 7).

Role of Lys64. Lys64 is a homologue of the general acidic Lys in the active site of OMPDC. On the basis of the available structures, we predict that Lys64, together with Asp67, stabilizes and restricts the *cis* geometry of the enediolate intermediate in the KGPDC-catalyzed reaction. Accordingly, we sought experimental evidence of this proposed role for Lys64 in the KGPDC-catalyzed reaction.

We were unable to perform NMR investigations of reactions catalyzed by the K64A mutant in buffers containing D_2O because the protein precipitates during exchange of the solvent isotope. However, the mutant is stable in buffers containing H_2O; we determined its high-resolution structure in the presence of the hydroxamate analogue of the enediolate intermediate as described in the following paper. Accordingly, we "reversed" the identities of the hydrogen isotopes in our NMR experiments; i.e., we used appropriately deuterated substrates, performed the reactions in deuterium-depleted H_2O buffer, and used ^{2}H NMR spectroscopy to monitor the fate of substrate and solvent hydrogens in both the product exchange and decarboxylation reactions.

The ^{2}H NMR spectrum of L-[1-$^2H_2$]xylulose 5-phosphate is presented in Figure 8A. Wild-type KGPDC catalyzes exchange of the *pro*-1*S* deuterium of L-[1-$^2H_2$]xylulose 5-phosphate (Figure 8B). However, K64A does not catalyze detectable exchange, even in the presence of increased amounts of the mutant protein (data not shown). We attribute the lack of exchange by the K64A mutant to (1) the significantly weakened stabilization of the enediolate intermediate and/or (2) an altered geometry of the intermediate or product relative to His136 and the proximal water molecule. In contrast to structures of other mutants, structures

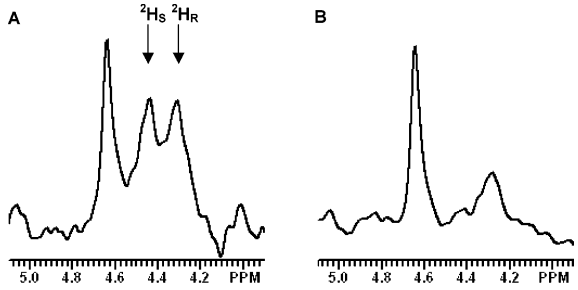

FIGURE 8: ^2H NMR spectra of L-[1-$^2H_2$]xylulose 5-phosphate obtained before (A) and after (B) incubation with wild-type KGPDC.

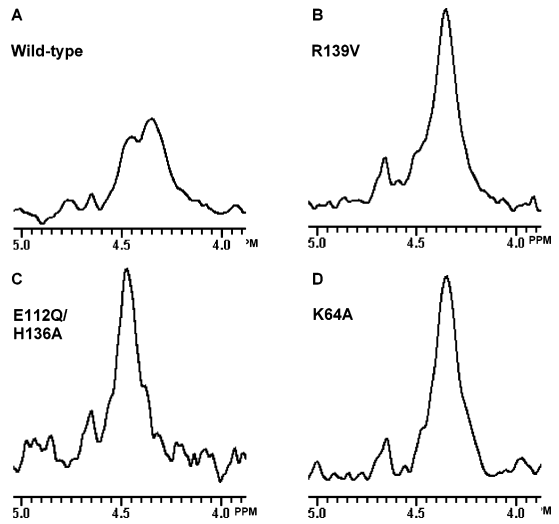

FIGURE 9: ^2H NMR spectra of L-xylulose 5-phosphate obtained from the decarboxylation of [2-^2H]-3-keto-L-gulonate 6-phosphate in H_2O using (A) wild-type KGPDC, (B) R139V, (C) E112Q/H136A, and (D) K64A.

of the K64A mutant in the presence of both the hydroxamate analogue of the enediolate intermediate and the L-xylulose 5-phosphate product reveal that the structure of the active site is altered, presumably as a result of removal of a charged group in the proximity of many other charged groups.

Using wild-type KGPDC and [2-^2H]-3-keto-L-gulonate 6-phosphate as the substrate for decarboxylation in deuterium-depleted H_2O buffer, we observed the expected formation of a mixture of L-[1*R*-^2H]- and L-[1*S*-^2H]xylulose 5-phosphate (Figure 9A), the former being favored by approximately the same 2:1 ratio observed in the experiments summarized in Figure 5A in which the incorporation of solvent deuterium was studied and monitored by ^1H NMR spectroscopy (^1H and ^2H are located in opposite positions, so the absolute configurations of C1 are opposite in the two experiments). We also used this experimental protocol to examine the reactions catalyzed by the R139V (Figure 9B) and E112Q/H136A (Figure 9C) mutants; as expected, these were accompanied by stereospecific incorporation of solvent protium to yield L-[1*R*-^2H]- and L-[1*S*-^2H]xylulose 5-phosphate, respectively.

With the K64A mutant, we observed predominant formation of L-[1*R*-^2H]xylulose 5-phosphate (Figure 9D); due to the line widths of ^2H NMR resonances, we cannot accurately determine whether the reaction is stereospecific. In any event, this product is the result of protonation on the *si*-face of C1 of the enediolate intermediate, as observed for wild-type KGPDC. The structures of the mutant suggest that the enediolate intermediate likely will be oriented toward His136 rather than the associated water molecule, with the predominant formation of L-[1*R*-^2H]xylulose 5-phosphate possibly explained by direct transfer of a solvent-derived hydrogen from His136.

The stability of the K64A substitution was enhanced when present with other substitutions in the same polypeptide, including K64A/R139V, K64A/E112Q/H136A, and K64A/E112A/H136A/R139V, thereby allowing us to examine the effect of the K64A substitution on the geometry of the enediolate intermediate using formaldehyde as the electrophilic probe. The same L-hex-3-ulose 6-phosphate aldol product was observed in each of these multiple mutants (data not shown). Although our structural evidence suggests a role for Lys64 in stabilizing the enediolate intermediate, that the same aldol product is produced in the presence of formaldehyde by mutants containing K64A suggests that Lys64 does not play a major role in enforcing the *cis* geometry for the enediolate intermediate.

Taken together, these experiments and the insights gained from the available structures are consistent with Lys64 stabilizing the *cis*-enediolate intermediate instead of functioning as a general acid to deliver a solvent-derived proton to the intermediate to generate the L-xylulose 5-phosphate product.

The following paper (*22*) describes structural studies of the K64A, H136A, E112Q, and E112Q/H1436A mutants complexed with L-threonohydroxamate 4-phosphate, an analogue of the *cis*-1,2-enediolate intermediate, that support the interpretations of the experiments reported in this paper.

CONCLUSIONS

OMPDC is a ubiquitous enzyme required for pyrimidine biosynthesis. In contrast, KGPDC is encoded by only the genomes of microorganisms that can utilize L-ascorbate as a carbon source, and HPS is encoded by only the genomes of microorganisms that assimilate formaldehyde by the aldol reaction with D-ribulose 5-phosphate. For this reason, we hypothesize that an OMPDC was the progenitor for the OMPDC suprafamily.

In mechanistically diverse superfamilies, conserved active site functional groups participate in a partial reaction shared by all members of the superfamily (*2*). In the case of the enolase superfamily, the ligands for an essential Mg^{2+} as well as at least one acid or base catalyst are conserved to allow an initial enolization of the carbon acid substrate; the second partial reaction in which the enolate intermediate is directed to product is not conserved. In contrast, despite the remarkable conservation of active site functional groups in OMPDC and KGPDC, their reaction mechanisms share no conserved functional features. The OMPDC-catalyzed reaction likely proceeds without the formation of a vinyl anion intermediate; the KGPDC-catalyzed reaction involves stabilization of an enolate intermediate. Although both decarboxylation reactions involve exergonic proton delivery from the solvent to generate the product, the positions and identities of the acids that mediate these reactions are not conserved.

In OMPDC, a Lys residue located at the end of the third β-strand of the $(\beta/\alpha)_8$-barrel domain is the acid. In KGPDC, water molecules located on either face of the *cis*-enediolate

intermediate compete for protonation of the intermediate, with their acidities modulated by the proximity to the His136−Glu112 dyad on the *si*-face of C1 of the intermediate and Arg139 on the *re*-face (Figure 3); His136 and Arg139 are located at the end of the sixth β-strand. The *cis*-enediolate intermediate is stabilized by direct interactions with three groups: Lys64, the homologue of the general acid in OMPDC, the essential Mg^{2+}, and Asp67. We conclude that Nature has followed an opportunistic pathway in the expected recruitment of an OMPDC progenitor to catalyze the mechanistically distinct reaction catalyzed by KGPDC.

Finally, enzyme-catalyzed reactions of carbon acids involving enediolate anion intermediates normally are both stereospecific and catalyzed by a protein-derived functional group. Our conclusion that two active site water molecules, not a single active site protein-derived functional group, compete as the general acid catalysts in the decarboxylation reaction may provide support for the recent divergence of KGPDC from OMPDC. Selective pressure for stereospecific protonation of the intermediate by a protein-derived functional group may not yet have occurred in its evolution to catalytic "perfection" (*21*); the value of k_{cat}/K_m ($\sim 10^5$ M^{-1} s^{-1}, Table 1) is smaller than that expected for a diffusion-controlled reaction, and delivery of a solvent-derived proton to the enediolate intermediate is not the rate-limiting step (the solvent deuterium isotope effect for wild-type KGPDC is 1.2; W. S. Yew and J. A. Gerlt, unpublished observations). Perhaps future selective pressure to enhance the efficiency of the KGPDC-catalyzed reaction will result in stereospecific protonation of the *cis*-enediolate intermediate by a protein-derived functional group.

REFERENCES

1. Yew, W. S., and Gerlt, J. A. (2002) Utilization of L-Ascorbate by *Escherichia coli* K-12: Assignments of Functions to Products of the yjf-sga and yia-sgb Operons, *J. Bacteriol. 184*, 302−306.
2. Gerlt, J. A., and Babbitt, P. C. (2001) Divergent Evolution of Enzymatic Function: Mechanistically Diverse Superfamilies and Functionally Distinct Suprafamilies, *Annu. Rev. Biochem. 70*, 209−246.
3. Wise, E., Yew, W. S., Babbitt, P. C., Gerlt, J. A., and Rayment, I. (2002) Homologous $(\beta/\alpha)_8$-barrel enzymes that catalyze unrelated reactions: orotidine 5′-monophosphate decarboxylase and 3-keto-L-gulonate 6-phosphate decarboxylase, *Biochemistry 41*, 3861−3869.
4. Gerlt, J. A., and Raushel, F. M. (2003) Evolution of function in $(\beta/\alpha)_8$-barrel enzymes, *Curr. Opin. Chem. Biol. 7*, 252−264.
5. Traut, T. W., and Temple, B. R. (2000) The chemistry of the reaction determines the invariant amino acids during the evolution and divergence of orotidine 5′-monophosphate decarboxylase, *J. Biol. Chem. 275*, 28675−28681.
6. Begley, T. P., Appleby, T. C., and Ealick, S. E. (2000) The structural basis for the remarkable catalytic proficiency of orotidine 5′-monophosphate decarboxylase, *Curr. Opin. Struct. Biol. 10*, 711−718.
7. Miller, B. G., and Wolfenden, R. (2002) Catalytic proficiency: the unusual case of OMP decarboxylase, *Annu. Rev. Biochem. 71*, 847−885.
8. Sievers, A., and Wolfenden, R. (2002) Equilibrium of formation of the 6-carbanion of UMP, a potential intermediate in the action of OMP decarboxylase, *J. Am. Chem. Soc. 124*, 13986−13987.
9. Appleby, T. C., Kinsland, C., Begley, T. P., and Ealick, S. E. (2000) The crystal structure and mechanism of orotidine 5′-monophosphate decarboxylase, *Proc. Natl. Acad. Sci. U.S.A. 97*, 2005−2010.
10. Wu, N., Mo, Y., Gao, J., and Pai, E. F. (2000) Electrostatic stress in catalysis: structure and mechanism of the enzyme orotidine monophosphate decarboxylase, *Proc. Natl. Acad. Sci. U.S.A. 97*, 2017−2022.
11. Miller, B. G., Hassell, A. M., Wolfenden, R., Milburn, M. V., and Short, S. A. (2000) Anatomy of a proficient enzyme: the structure of orotidine 5′-monophosphate decarboxylase in the presence and absence of a potential transition state analog, *Proc. Natl. Acad. Sci. U.S.A. 97*, 2011−2016.
12. Wise, E., Yew, W. S., Gerlt, J. A., and Rayment, I. (2003) Structural evidence for a 1,2-enediolate intermediate in the reaction catalyzed by 3-keto-L-gulonate 6-phosphate decarboxylase, a member of the orotidine 5′-monophosphate decarboxylase suprafamily, *Biochemistry 42*, 12133−12142.
13. Datsenko, K. A., and Wanner, B. L. (2000) One-step inactivation of chromosomal genes in *Escherichia coli* K-12 using PCR products, *Proc. Natl. Acad. Sci. U.S.A. 97*, 6640−6645.
14. Hamilton, G. A., and Westheimer, F. H. (1959) On the mechanism of the enzymatic decarboxylation of acetoacetate, *J. Am. Chem. Soc. 81*, 6332−6333.
15. Fridovich, I., and Westheimer, F. H. (1962) On the mechanism of the enzymatic decarboxylation of acetoacetate II, *J. Am. Chem. Soc. 84*, 3208−3209.
16. Kobes, R. D., Simpson, R. T., Vallee, R. L., and Rutter, W. J. (1969) A functional role of metal ions in a class II aldolase, *Biochemistry 8*, 585−588.
17. Hall, D. R., Leonard, G. A., Reed, C. D., Watt, C. I., Berry, A., and Hunter, W. N. (1999) The crystal structure of *Escherichia coli* class II fructose-1,6-bisphosphate aldolase in complex with phosphoglycolohydroxamate reveals details of mechanism and specificity, *J. Mol. Biol. 287*, 383−394.
18. Rose, I. A., and O'Connell, E. L. (1960) Stereospecificity of the sugar−phosphate isomerase reactions; a uniformity, *Biochim. Biophys. Acta 42*, 159−160.
19. Piccirilli, J. A., Rozzell, J. D., and Benner, S. A. (1987) The stereospecificity of oxalacetate decarboxylase: a stereochemical imperative? *J. Am. Chem. Soc. 109*, 8084−8085.
20. Rozzell, J. D., and Benner, S. A. (1984) Stereochemical imperative in enzymic decarboxylations. Stereochemical course of the decarboxylation catalyzed by acetoacetate decarboxylase, *J. Am. Chem. Soc. 106*, 4937−4941.
21. Albery, W. J., and Knowles, J. R. (1976) Evolution of enzyme function and the development of catalytic efficiency, *Biochemistry 15*, 5631−5640.
22. Wise, E. L., Yew, W. S., Gerlt, J. A., and Rayment, I. (2004) *Biochemistry 43*, 6438−6446.

BI049741T